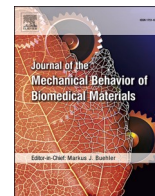




Contents lists available at ScienceDirect

## Journal of the Mechanical Behavior of Biomedical Materials

journal homepage: [www.elsevier.com/locate/jmbbm](http://www.elsevier.com/locate/jmbbm)

## Dimensional accuracy and simulation-based optimization of polyolefins and biocopolyesters for extrusion-based additive manufacturing and steam sterilization.

Felix Burkhardt<sup>a,\*</sup>, Carl G. Schirmeister<sup>b,c</sup>, Christian Wesemann<sup>a</sup>, Lukas Baur<sup>a</sup>, Kirstin Vach<sup>d</sup>, Massimo Nutini<sup>e</sup>, Erik H. Licht<sup>c</sup>, Marc C. Metzger<sup>f</sup>, Rolf Mülhaupt<sup>b,g</sup>, Benedikt C. Spies<sup>a</sup>

<sup>a</sup> Medical Center – University of Freiburg, Center for Dental Medicine, Department of Prosthetic Dentistry, Faculty of Medicine, University of Freiburg, Hugstetter Str. 55, 79106, Freiburg, Germany

<sup>b</sup> Freiburg Materials Research Center FMF and Institute for Macromolecular Chemistry, Albert-Ludwigs-University Freiburg, Stefan-Meier-Str. 21, 79104, Freiburg, Germany

<sup>c</sup> Basell Sales & Marketing B.V., LyondellBasell Industries, Industriepark Höchst, 65926, Frankfurt a.M, Germany

<sup>d</sup> Medical Center - University of Freiburg, Institute for Medical Biometry and Statistics, Faculty of Medicine, University of Freiburg, Stefan-Meier-Str. 26, 79104, Freiburg, Germany

<sup>e</sup> Basell Poliolefine Italia Srl, LyondellBasell Industries, P. le Privato G. Donegani 12, 44122, Ferrara, Italy

<sup>f</sup> Medical Center – University of Freiburg, Center of Dental Medicine, Department of Oral and Maxillofacial Surgery, University of Freiburg, Hugstetter Str. 55, 79106, Freiburg, Germany

<sup>g</sup> Sustainability Center Freiburg, Ecker-Str. 4, 79104, Freiburg, Germany

## ARTICLE INFO

## Keywords:

Additive manufacturing  
Medical 3D printing  
Fused filament fabrication  
Simulation-based optimization  
Finite element simulation

## ABSTRACT

Polyolefins exhibit robust mechanical and chemical properties and can be applied in the medical field, e.g. for the manufacturing of dentures. Despite their wide range of applications, they are rarely used in extrusion-based printing due to their warpage tendency. The aim of this study was to investigate and reduce the warpage of polyolefins compared to commonly used filaments after additive manufacturing (AM) and sterilization using finite element simulation. Three types of filaments were investigated: a medical-grade polypropylene (PP), a glass-fiber reinforced polypropylene (PP-GF), and a biocopolyester (BE) filament, and they were compared to an acrylic resin (AR) for material jetting. Square specimens, standardized samples prone to warpage, and denture bases ( $n = 10$  of each group), as clinically relevant and anatomically shaped reference, were digitized after AM and steam sterilization (134 °C). To determine warpage, the volume underneath the square specimens was calculated, while the deviations of the denture bases from the printing file were measured using root mean square (RMS) values. To reduce the warpage of the PP denture base, a simulation of the printing file based on thermomechanical calculations was performed. Statistical analysis was conducted using the Kruskal-Wallis test, followed by Dunn's test for multiple comparisons. The results showed that PP exhibited the greatest warpage of the square specimens after AM, while PP-GF, BE, and AR showed minimal warpage before sterilization. However, warpage increased for PP-GF, BE and AR during sterilization, whereas PP remained more stable. After AM, denture bases made of PP showed the highest warpage. Through simulation-based optimization, warpage of the PP denture base was successfully reduced by 25%. In contrast to the reference materials, PP demonstrated greater dimensional stability during sterilization, making it a potential alternative for medical applications. Nevertheless, reducing warpage during the cooling process after AM remains necessary, and simulation-based optimization holds promise in addressing this issue.

\* Corresponding author. Medical Center - University of Freiburg, Center for Dental Medicine, Department of Prosthetic Dentistry, Faculty of Medicine University of Freiburg, Hugstetter Str. 55, 79106, Freiburg, Germany.

E-mail address: [felix.burkhardt@uniklinik-freiburg.de](mailto:felix.burkhardt@uniklinik-freiburg.de) (F. Burkhardt).

<https://doi.org/10.1016/j.jmbbm.2024.106507>

Received 31 January 2024; Received in revised form 4 March 2024; Accepted 12 March 2024

Available online 13 March 2024

1751-6161/© 2024 The Authors. Published by Elsevier Ltd. This is an open access article under the CC BY license (<http://creativecommons.org/licenses/by/4.0/>).

## 1. Introduction

The use of additive manufacturing (AM) techniques in the medical field shows great promise for personalized patient treatments (Aimar et al., 2019; Hoang et al., 2016). In this context, the most commonly used AM techniques are stereolithography (SLA), digital light processing (DLP), and material jetting (Ligon et al., 2017; Revilla-León et al., 2020). These techniques enable the production of high-precision objects such as surgical guides for oral implants (Ma et al., 2018) and craniomaxillofacial surgeries (Ballard et al., 2020). However, AM with light-curing resins can be time-consuming, expensive, and challenging to operate. In contrast, material extrusion AM, also known as fused filament fabrication (FFF) or fused deposition modeling (FDM), represents a simple and cost-effective method (Davis et al., 2017; Ligon et al., 2017). In this process, thermoplastic filaments are melted in a heated nozzle and deposited layer by layer on a heating platform. The commonly used materials for FFF are amorphous polymers like acrylonitrile-butadiene-styrene copolymers (ABS) and polycarbonates or semi-crystalline thermoplastics like polylactide acid (PLA) (Ligon et al., 2017; Mohan et al., 2017). However, these materials often exhibit a lower degree of crystallinity, low crystallization rates, and limited chemical resistance.

Polyolefins such as polyethylene and polypropylene dominate by almost two-thirds the global plastics production (Stürzel et al., 2016). From a chemical perspective, polyolefins belong to the group of hydrocarbons with high molar mass, high purity, and low allergy potential (Chung, 2013). Their solvent-free catalytic polymerization and easy recyclability make them cost- and resource-efficient materials (Tabone et al., 2010; Mühlaupt, 2013; Vidakis et al., 2020a). Furthermore, polyolefins possess high mechanical (Vidakis et al., 2020b) and chemical robustness, as well as low water absorption, which makes them widely used in the medical environment, e.g. in the form of tubes, syringes, and even acetabular implants (Musib, 2012). However, due to their semi-crystalline nature, polyolefins are rarely used in extrusion-based AM. The cooling process during solidification, which is caused by crystallization, leads to a reduction in volume and consequently to considerable shrinkage and warpage of the polymer (Bachhar et al., 2020; Wang et al., 2007). Researchers have attempted to reduce warpage of extrusion-based printed polypropylene by optimizing printing parameters, pathways, and adhesion to the build platform (Carneiro et al., 2015; Winter et al., 2022). However, these adjustments often result in reduced mechanical properties of the printed polypropylene objects. Additionally, the reduction of crystallinity through the use of ethylene-propylene copolymers leads to decreased warpage which was associated with a lower heat deflection and melting temperature (Spoerk et al., 2020). This limitation prevents the printed objects from being exposed to high temperatures, which hampers certain applications, e.g., steam sterilization. Another approach to improve dimensional stability is the addition of organic and inorganic fillers (Bertolino et al., 2021; Kaynak et al., 2018; Spoerk et al., 2019). It is often the case that the mechanical properties of 3D-printed parts are dependent on the printing direction, especially when using fillers with an anisotropic shape (Winter et al., 2022). Regardless of their morphology and aspect ratios, the fillers must be aligned in the direction in which the polymer strand is deposited. In order to develop polypropylene filaments with improved mechanical characteristics, polypropylene filaments with tungsten carbide ceramic and glass microparticles were investigated, which showed enhanced tensile and flexural strength (Moutsopoulou et al., 2023; Petousis et al., 2023). It was also demonstrated that polypropylene nanocomposites with different types of additives such as aluminum oxide, silicon dioxide and titanium dioxide showed enhanced mechanical properties (Vidakis et al., 2021a, 2021b, 2022b).

Another approach to improve the dimensional stability is represented by a catalytic multi-stage polymerization using glass fiber-reinforced polypropylene composites (Schirmeister et al., 2021). In a

single reactor or reactor cascade, both polypropylene polymerization and the integration of nanophase-separated reactor blends (poly(ethylene-co-1-olefin)) are achieved. This reduces the risk of residual stresses from thermal shrinkage being frozen and subsequently released at elevated temperatures, leading to warpage. Another versatile attempt to minimize distortion is to use pre-deformed CAD (computer-aided design) files (Nath et al., 2020; Schmutzler et al., 2016). These CAD designs are based on thermomechanical calculations of the underlying material, printing parameters, and object geometries (Burkhardt et al., 2020).

Denture bases are increasingly being produced using additive techniques and the manufacturing of dentures using FFF has been examined in laboratory investigations (Deng et al., 2023). The use of polyolefins for this purpose is of interest because the materials are robust and inexpensive and they represent a low allergy potential. For a variety of applications of FFF-printed parts in the medical field, such as surgical guides or instruments, sterilization is necessary to meet hygiene and safety standards. Steam sterilization of dentures is not a frequently applied method but represents a simple approach to clean dentures in the field of geriatric dentistry. The above literature shows that several approaches can lead to improved mechanical properties and dimensional stability. However, little is known about the compatibility of polypropylene-printed parts with steam sterilization. To the author's best knowledge, extrusion-based printed medical-grade polypropylene and glass fiber-reinforced polypropylene composite for clinical use after steam sterilization have not yet been investigated. Furthermore, extrusion-based fabrication and accuracy analysis of denture bases using polyolefins and simulation-based optimization of this clinically relevant geometry have not yet been described in the literature. The application of extrusion-based printed denture bases using polyolefins and their cleaning by means of steam sterilization could represent a biocompatible and cost-effective alternative in the field of geriatric dentistry. For the objective of this study, the dimensional accuracy after AM and the effects of steam sterilization of medical-grade polypropylene and a low-warpage glass-fiber reinforced polypropylene were investigated and compared to a commonly used biopolyester filament that typically exhibits good processing properties in extrusion-based 3D printing, such as low warpage, but limited chemical and physical robustness as well as a medically approved resin for material jetting. A specific focus is given to the use of polypropylene in order to leverage its excellent chemical robustness, its high purity, its low water absorption during steam sterilization and its outstanding eco-balance for medial 3D printing (Chung, 2013; Mühlaupt, 2013; Tabone et al., 2010). For this purpose, square specimens, standardized samples prone to warpage, and denture bases were digitized using a coordinate measuring machine after AM and steam sterilization (134 °C). To determine warpage, the volume underneath the square specimens was calculated, while the deviations of the denture bases from the printing file were measured with an inspection software using root mean square (RMS) values. A thermal characterization of the materials and evaluation of crystallinity was conducted using differential scanning calorimetry. To reduce the warpage of the PP denture base, a simulation of the printing file based on thermomechanical calculations was performed.

## 2. Materials and methods

### 2.1. Evaluated materials

A medical-grade semi-crystalline polypropylene injection molding granulate (plain heterophasic PP for healthcare applications, *Purell* type, LyondellBasell Industries B.V., Rotterdam, The Netherlands, MFR = 15 g (10 min)<sup>-1</sup>) with certified biocompatibility according to United States Pharmacopeia (USP) Class VI served as the feedstock for the extrusion of a medical polypropylene filament (PP). Another polypropylene material was evaluated, based on *Beon3D* PPG 2290, which contained nanophase-separated *Catalloy*-based polypropylene pellets and 25 wt% short glass

fibers (PP-GF) (supplied by LyondellBasell) without specific addition except for <1 wt % coupling agent to ensure adhesion between the PP and the glass fibers (Schirmeister et al., 2021). As previously published, the PP-GF exhibits a very low tendency to warp due to its nanophase-separated rubber content (Ethylene-Propylene Copolymer) and the glass fibers (Schirmeister et al., 2021). Furthermore, a commonly used biocopolyester (BE) blend based on the biopolymers poly lactide acid (PLA), polybutylene adipate terephthalate (PBAT), and polyhydroxyalkanoate (PHA) (GreenTec Pro, Extrudr, Lauterbach, Austria) was investigated. This BE filament was compostable according to EN 13432:2002 (2002). The material composition of this commercial filament was investigated in a previous publication (Burkhardt et al., 2022a,b). For comparison, a commercially available photo-curable acrylic resin used in the medical field (AR, MED610, StrataSys, Eden Prairie, USA) was selected for PolyJet AM.

## 2.2. Polymer melt processing

The PP filament was produced from pellets using a twin-screw extruder (Teach-Line™, ZK 25 T, Collin, Ebersberg, Germany) at 180 °C and 45 rpm, with a 3.3 mm diameter, a water-cooling system, and a winding unit (take-off speed 90 mm s<sup>-1</sup>). The PP-GF filament was also extruded from pellets using the same twin-screw extruder at 180 °C and 35 rpm equipped with a 3.0 mm nozzle. The polymer strands were pulled of (65–69 mm s<sup>-1</sup>) and wrapped onto a spool. BE was commercially available as a filament for extrusion-based printing.

## 2.3. Additive manufacturing of test specimens

Computer-aided design (CAD) files were created using Ultimaker Cura 4.0.0 software and FFF was conducted using an Ultimaker S5 printer which was equipped with round steel nozzles with 0.5 mm diameter (nozzle temperature of 220 °C, printing bed temperature of 60 °C) and a printing speed of 35 mm s<sup>-1</sup>. The layer thickness was 0.2 mm and the filling degree was 100 % for all printed specimens using FFF. The 3D printing parameters were selected to allow for reliable results in terms of printability and mechanical part properties for both PP-based materials according to optimizations published previously (Burkhardt et al., 2022a,b; Schirmeister et al., 2021). All of the extrusion based printed specimens were annealed at 80 °C for 24 h under vacuum conditions. For group AR, test specimens were printed with a PolyJet Printer (Objet Eden260VS™, StrataSys). The printing quality was set to high, the surface was printed matte, and the infill rate was 100 %. After removing the support structures, printed parts were dried in the open air for 2 h at room temperature. In order to accurately determine warpage between the different polymers, a square specimen (10 × 10 cm) was chosen (n = 10 of each group), which tends to exhibit severe warpage due to its long and thin sides (Fig. 1). Furthermore, it requires a short printing time due to its low height of 2 mm (Spoerk et al., 2017). A denture base was selected for the evaluation of a geometry close to the

potential application in the dental field (n = 10 of each group). For the design of the denture base, an edentulous maxillary typodont model (B3–NH, Frasaco, Tettngang, Germany) was digitized with a laboratory scanner (3Shape E4, 3Shape, Copenhagen, Denmark). The denture base was designed (inLab CAD, Dentsply Sirona, Charlotte, North Carolina, USA) and a flat occlusal surface was created (Meshmixer, Autodesk, San Rafael, California, USA). The design of the denture base exhibits a large volume, is thicker compared to the square specimens, and requires dimensionally accurate fabrication for a proper fit on the patient.

## 2.4. Sterilization

All of the test specimens were cleaned in a washer-disinfector (PG 8536, Miele, Gütersloh, Germany) containing a liquid detergent (neodisher MediClean forte, Dr. Weigert AG, Zug, Switzerland) with washing at 55 °C for 10 min and disinfection at 90 °C for 5 min. Subsequently, the specimens were steam sterilized in an autoclave (Webeco, Series EC, Selmsdorf, Germany) at 134 °C for 5 min. The second evaluated sterilization protocol, which was additionally used for PP-GF and BE, included only steam sterilization at 121 °C for 20 min. In the field of geriatric dentistry, cleaning dentures using steam sterilization can be a cost-effective and simple method.

## 2.5. Warpage quantification

Square specimens and denture bases were digitized with a 3D coordinate measuring machine (VL-5000, Keyence, Osaka, Japan) after manufacturing (including annealing) and after sterilization. The optical coordinate measuring machine captured 16 million points with a measuring accuracy of ±10 μm and a repeatability of 2 μm (Keyence, 2024). Based on these measuring points, the measured object was generated as an STL file by the software associated with the coordinate measuring machine. In the case of the square specimens, this STL data set also included the areas below the struts caused by the warpage (Fig. 3). The volume of this object was determined in an inspection software (Geomagic Control X, 3D Systems, Rock Hill, USA). To obtain solely the resulting deviation caused by shrinkage and warpage, the volume of the original geometry STL file was subtracted from the measured volume. The scans of the denture bases were also imported into the inspection software (Geomagic Control X) and compared to the original STL using a local best-fit algorithm according to Gauss. The mean deviation was calculated according to the root mean square (RMS) value, and the orientation of the deviation was evaluated according to the negative and positive mean values. For visualization, the deviations were illustrated using a color map and a tolerance of ±100 μm indicating the positive and negative deviations. A deviation of ±100 μm appears within the range of denture base adaptation (Wang et al., 2021; Wemken et al., 2020).

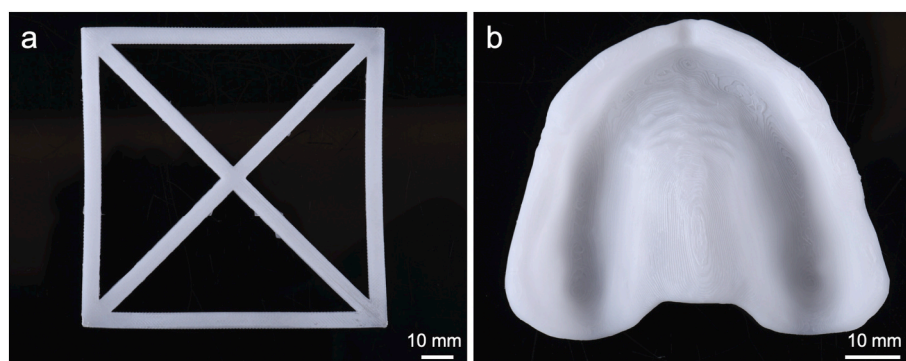
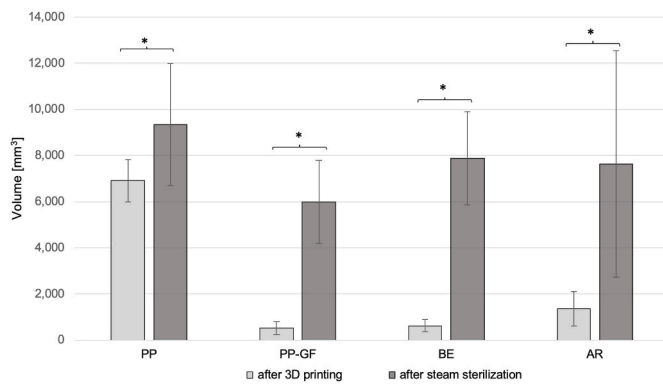


Fig. 1. Printed specimens: Rectangular square (a) and denture base (b) made of PP.



**Fig. 2.** Warpage of square specimens after additive manufacturing and after steam sterilization (134 °C) by visualization of the volume underneath warped specimens. Asterisks (\*) indicate significance ( $p < 0.05$ ) between the two evaluated time points of each group.

## 2.6. Differential scanning calorimetry (DSC)

Thermal characterization was conducted through DSC using a DSC 6200 F1 (Seiko, Chiba, Japan) at a heating rate of 10 K min<sup>-1</sup>.

## 2.7. Printing process simulation

To compensate for the inherent warping issues of PP group, thermomechanical calculations were performed to simulate the printing process based on the physical properties of the medical PP and its melt using Digimat-AM software and Marc finite element solver (both Hexagon AB, Stockholm, Sweden) (e-Xstream engineering, 2021). The mesh of the denture base consisted of cubic voxels, with edge lengths ranging from of 0.3–2 mm, resulting in about 520,000 elements for the finest mesh and 2960 elements for a coarser mesh. The optimization process used a mesh with a 0.5 mm voxel side and 120,000 elements since the results showed only minor differences compared to the finest mesh. The simulation process generated a counter-warped CAD file by subtracting the resulting deformation of the denture base from the original target geometry. Two different simulation methods, based on different modelling approaches were applied for warpage reduction (Inherent-Strain model; PP-IS; Thermo-Mechanical model, PP-TM) which were both available in the software. The term “inherent strain”, refers to all the strains that originate inside the material due to thermo-mechanical phenomena occurring in the process. The pre-processing phase involved a thermomechanical analysis carried out on several Reference Volumes Elements (RVE) under various process parameters, and the resulting strains were stored. The computed strains in this phase were dependent on the process conditions and the material data but not on the material history. During the calculation of the part, the results from the simulation of the RVE were retrieved and assembled to simulate the behavior of the layers.

On the other hand, the PP-TM model relies on the finite element analysis carried out with a finite element solver. In this case, the thermo-mechanics equation governing the behavior of each element during the process of progressive deposition of the layer was solved. This allowed taking into account time-dependent phenomena such as element cooling, properties, and plasticity, making it suitable for modeling creep and relaxation occurring in the process, e.g., during the final annealing phase. For the present case, generic characterization for injection molding process simulation was used. In particular, Prony series for temperature-dependent properties modeling based on the Williams–Landel–Ferry (WLF) equation were used to model the viscoelastic behavior, which was measured from creep tests executed at various temperatures (Williams et al., 1955). The related parameters were calibrated reproducing the variability of the elastic modulus with the

temperature in a 1D simulation on a RVE, executed with the software package Digimat-MF (Hexagon AB). For both optimized denture base models (PP-IS; PP-TM),  $n = 10$  samples of each group were evaluated.

## 2.8. Statistical analyses

The mean, median, and standard deviation were calculated for the descriptive analyses. Statistical analysis was performed using the Kruskal-Wallis test followed by Dunn’s test with Bonferroni-Correction for multiple comparisons. A statistical significance level was set to  $p < 0.05$ . The calculations were performed with the statistical software STATA 17.0 (StataCorp, College Station, Texas, USA).

## 3. Results

### 3.1. Warpage quantification

After AM and annealing of the square specimens, PP showed the highest warpage due to the largest enclosed volume below the square specimens ( $6906 \pm 915 \text{ mm}^3$ ) as typically observed for semicrystalline materials with a relatively high degree of crystallinity, whereas the other groups showed reduced warpage (PP-GF:  $513 \pm 277 \text{ mm}^3$ ; BE:  $617 \pm 267 \text{ mm}^3$ ; AR:  $1357 \pm 754 \text{ mm}^3$ ) (Fig. 2). No significant differences were observed between PP-GF, BE, and AR ( $P > 0.05$ ), while PP showed a significant increased warpage compared to the other groups ( $P < 0.01$ ). After steam sterilization at 134 °C, a significant increase in volume was observed for all groups (PP:  $9.342 \pm 2.649 \text{ mm}^3$ ; PP-GF:  $5.977 \pm 1.796 \text{ mm}^3$ ; BE:  $7.871 \pm 2.020 \text{ mm}^3$ ; AR:  $7.638 \pm 4.905 \text{ mm}^3$ ) (Figs. 2 and 3).

Compared with PP-GF, BE, and AR ( $P < 0.01$ ), the increase in warpage for group PP was comparatively small ( $P = 0.027$ ). Warping of the square specimens became visible by the corners bent upwards. The control group AR showed varying degrees of warpage resulting in a high standard deviation after steam sterilization ( $\pm 4.905 \text{ mm}^3$ ). The extrusion-based materials PP-GF and BE, which showed a high increase in warpage after steam sterilization at 134 °C, were additionally evaluated applying a modified steam sterilization protocol (121 °C; 20 min). Although both materials showed a significant increase in warpage again at 121 °C ( $P < 0.01$ ), the increase in warpage was smaller compared to the exposure at 134 °C (Fig. 4). PP-GF showed an increase of  $1247 \pm 725 \text{ mm}^3$  at 121 °C instead of  $5464 \pm 187 \text{ mm}^3$  at 134 °C ( $P = 0.045$ ). BE showed an increase of  $4.038 \pm 2.488 \text{ mm}^3$  at 121 °C instead of  $7.254 \pm 2.084 \text{ mm}^3$  at 134 °C ( $P = 0.751$ ). In both sterilization protocols, standard deviation increased after steam sterilization for all evaluated groups. This indicates that warpage caused by steam sterilization is differently pronounced for the evaluated samples within one group. Dimensional accuracy was also evaluated using the geometry of a denture base, which is a potential application for the evaluated materials. The intaglio surface of a denture base was investigated in total as well as in four different areas (Fig. 5).

Similar to the square specimens, PP showed the highest deviation after additive manufacturing (RMS:  $0.48 \pm 0.01$ ) compared to PP-GF ( $0.15 \pm 0.02$ ), BE ( $0.01 \pm 0.01$ ) and AR ( $0.06 \pm 0.01$ ) ( $p < 0.001$ ) (Figs. 6 and 7). The denture bases made of PP-GF, BE and AR showed no significant difference among themselves after AM ( $P < 0.05$ ). Steam sterilization at 134 °C resulted in a significant dimensional change for all evaluated groups ( $P < 0.05$ ). Nevertheless, the denture bases showed a smaller increase in warpage after steam sterilization at 134 °C than the square specimens, proving that the square design is a very sensitive specimen to detect warpage. With regard to the different areas of the intaglio surface of the denture, a significantly increased warpage of PP to the other groups was observed in the palatal region, in the region of the alveolar ridge, and in the dorsal area ( $P < 0.001$ ) (Fig. 6). In these regions, the PP-GF, BE, and AR groups showed no significant differences among themselves ( $P > 0.05$ ). In the lateral region of the denture base, only significant differences between PP and AR were calculated ( $p = 0.01$ ).

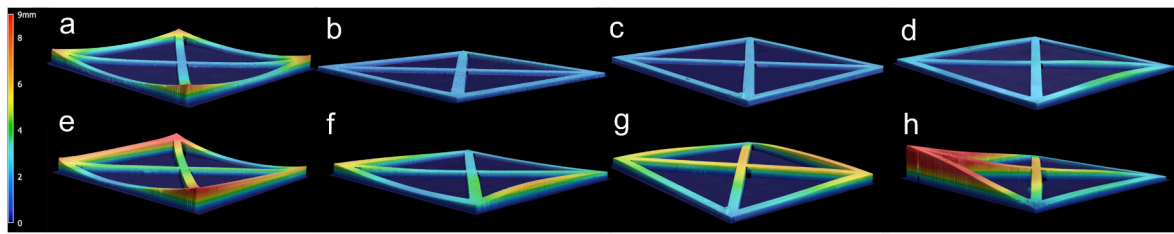


Fig. 3. Exemplary images visualizing the warpage of square specimens made of PP (a, e), PP-GF (b, f), BE (c, g), and AR (d, h) after additive manufacturing (a-d) and after 134 °C steam sterilization (e-h). (color artwork).

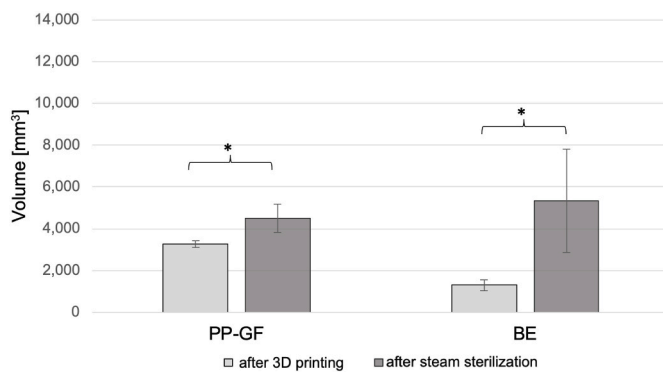


Fig. 4. Warpage of square specimens (PP-GF and BE) after additive manufacturing and steam sterilization (121 °C) by visualization of the volume underneath warped specimens. Asterisks (\*) indicate significance ( $p < 0.05$ ) between the two evaluated time points of each group.

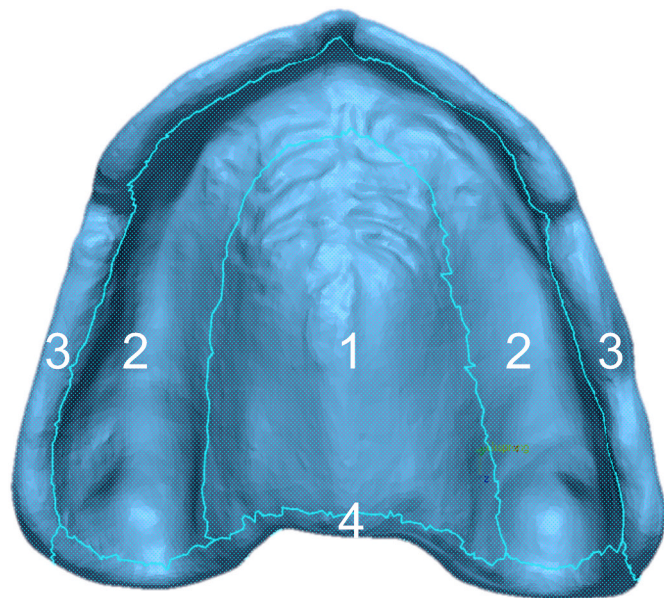


Fig. 5. Intaglio surface of a denture base indicating the evaluated areas: (1) palate; (2) alveolar ridge; (3) lateral, and (4) dorsal marginal ridges.

### 3.2. DSC

The extrusion-based materials (PP, PP-GF, BE) were measured for thermal characterization of after AM and after steam sterilization (134 °C) (Table 1). BE exhibited three melting points relating to PLA, PBAT and PHA (Burkhardt et al., 2022a,b). With regard to the polyolefin materials, PP-GF showed an overall reduced melt enthalpy compared to PP indicating the significantly reduced crystallinity. All materials

exhibit an increasing melting enthalpy after steam sterilization compared to the analysis after AM. However, the increase in warpage and the increase in crystallinity correlate only to a limited extent, which indicates that the elevated temperature of steam sterilization essentially releases inherent material stresses that have a significant influence on warpage.

### 3.3. Printing process simulation

Based on the obtained data, two models (PP-IS; PP-TM) were created to reduce the warpage of the denture bases during extrusion based printing of PP (Fig. 8). Both models showed reduced deviations from the original target (CAD file) compared to PP (Fig. 9). The RMS value of the PP-IS model was  $0.37 \pm 0.01$  (-23% versus original CAD file), and of the PP-TM model  $0.36 \pm 0.02$  (-25% versus original CAD file); whereas the RMS value of the non-optimized PP was  $0.48 \pm 0.01$ . The p-value comparing PP and PP-IS was 0.43 and comparing PP and PP-TM 0.07. When examining the individual regions of the simulation-based optimized denture bases, a significantly reduced RMS was observed in the area of the alveolar ridge compared to PP ( $P = 0.03$ ). The lowest RMS was described for both models (PP-TM; PP-IS) in the palatal region, whereas they showed the highest RMS in the dorsal margin region.

Four loops of optimization were used for the PP-TM approach, while only two optimization loops were carried out for the PP-IS approach, since in that case the solution proved to be oscillating, and no further improvements were achieved in subsequent loops.

## 4. Discussion

FFF represents a simple and cost-effective technology for the manufacturing of customized devices for patients in the medical sector (Lüchtenborg et al., 2021; Gielisch et al., 2022; Hada et al., 2023). Material selection is of great importance for achieving robust and long-term stable results. Polyolefins, such as polypropylene, exhibit low water absorption, favorable mechanical properties, and low allergic potential due to their comparatively increased crystalline properties, distinguishing them from commonly used PLA or ABS-based biocopolyesters (Malpass and Band, 2012).

The investigated PP filament was extruded from a medically approved (USP VI) injection molding granulate (Burkhardt et al., 2020), and no cytotoxic effects were observed in gingiva keratinocytes according to ISO 10993 after extrusion-based printing (Burkhardt et al., 2022a,b). This indicates that the processed filament can be applied intraorally without assuming cytotoxic consequences. However, polyolefin-based materials have rarely been used in FFF to date, as they pose difficulties in printing, resulting in shrinkage and warpage due to crystallization during the cooling process (Fischer, 2013; Spoerk et al., 2017; Stürzel et al., 2016; Wang et al., 2007). In the present study, PP showed the highest warpage compared to the other groups, regardless of the printing geometry. In contrast, the glass-fiber reinforced composite (PP-GF) exhibited significantly reduced warpage during AM of the square test specimens and the denture bases. The reduced shrinkage during the cooling process in PP-GF can be attributed to the reduced

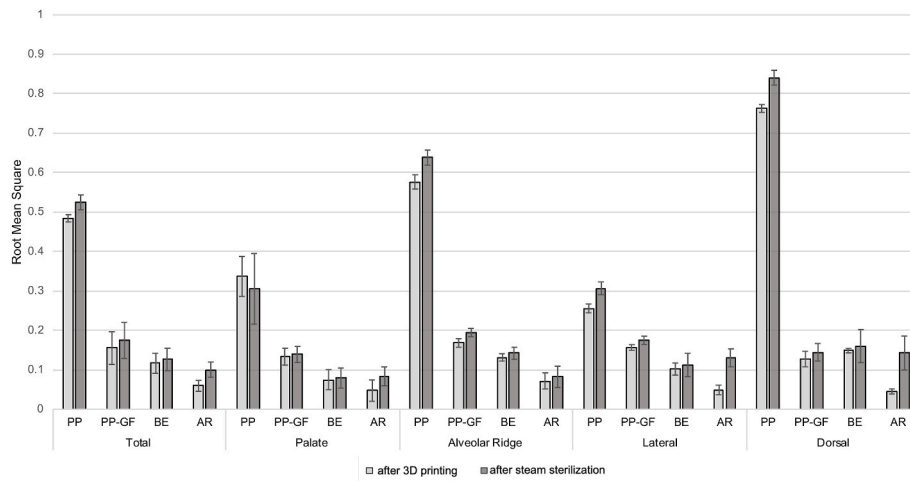


Fig. 6. Root Mean Square Values of additively manufactured denture bases after additive manufacturing and after steam sterilization.

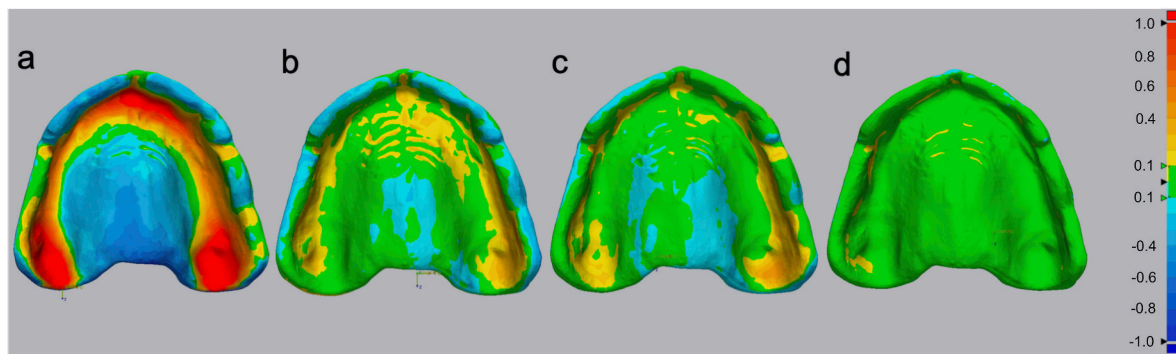


Fig. 7. Target-actual comparison of the intaglio surface of additively manufactured denture bases made of (a) PP, (b) PP-GF, (c) BE, and (d) AR. (color artwork).

Table 1  
DSC analyses of the evaluated extrusion-based materials.

	After additive manufacturing (1. Heating cycle)		After steam sterilization (134 °C) (1. Heating cycle)	
	T <sub>m</sub> [°C]	ΔH [J/g]	T <sub>m</sub> [°C]	ΔH [J/g]
PP	167	67	168	72
PP-GF	163	33	163	36
BE	175	37	176	37
			158	5
	113	5	113	5

crystallinity of the reactor blends without affecting the crystallinity of the PP polymer matrix (Schirmeister et al., 2021). The observed shrinkage of the test specimens was within the range of the amorphous or low-crystalline materials commonly used in FFF, such as BE. The PolyJet technique allowed for the manufacturing of precise and dimensionally accurate specimens, consistent with the existing literature regarding the fabrication of polymers using light-curing printing techniques (Németh et al., 2023; Revilla-León et al., 2020). No significant differences in the accuracy of dentures could be determined for this technology compared to other common processes (digital light processing, conventional injection molding, etc.) (Schubert et al., 2022).

All of the extrusion-based printed objects were annealed at 80 °C for 24 h under vacuum conditions as a post-fabrication method after AM. Annealing reorganizes the amorphous and poorly organized crystalline areas (Park et al., 2004), leading to increased thermal and mechanical stability by reducing internal stress (Díez-Rodríguez et al., 2020; Liao et al., 2019). The applied annealing protocol allowed for warpage

quantification of the specimens independent of the printing conditions (Schirmeister et al., 2021). In the present study, a mild annealing protocol was chosen, in which the applied temperature was significantly lower than the temperature of the polymer melt, requiring the annealing process to be extended accordingly. Since the test specimens were solely measured after AM and annealing, it cannot be assessed whether the annealing process led to a dimensional change of the two polyolefin-based materials (PP; PP-GF). In a comparable study, it was observed that annealing of BE caused a significant dimensional change in addition to an increase in crystallization, whereas modification of BE with fillers and nucleating agents reduced warpage during annealing (Burkhardt et al., 2022a,b). However, the applied annealing protocol comprised higher temperatures for a shorter period of time (max. 140 °C, 2.5 h in total, no vacuum). Further studies should consider the influence of the applied annealing protocol on the evaluated polyolefin-based materials (PP; PP-GF).

Steam sterilization may represent a simple approach to clean dentures in the field of geriatric dentistry. Furthermore, the investigated materials were not only intended for use as a denture base but also for other tailored medical applications. Therefore, the influence of steam sterilization (e.g. for applications in the surgical field) on the dimensional stability was evaluated. In the present study, steam sterilization at 134 °C for 5 min resulted in a significant dimensional change of all of the investigated materials. However, with regard to the square specimens, the volume change below the square specimens of PP-GF, BE, and AR was more pronounced compared to PP. This difference could be attributed to the comparatively increased thermal resistance of PP due to the enhanced degree of crystallization and the complete crystallization as well as the complete release of inherent stresses in the course of

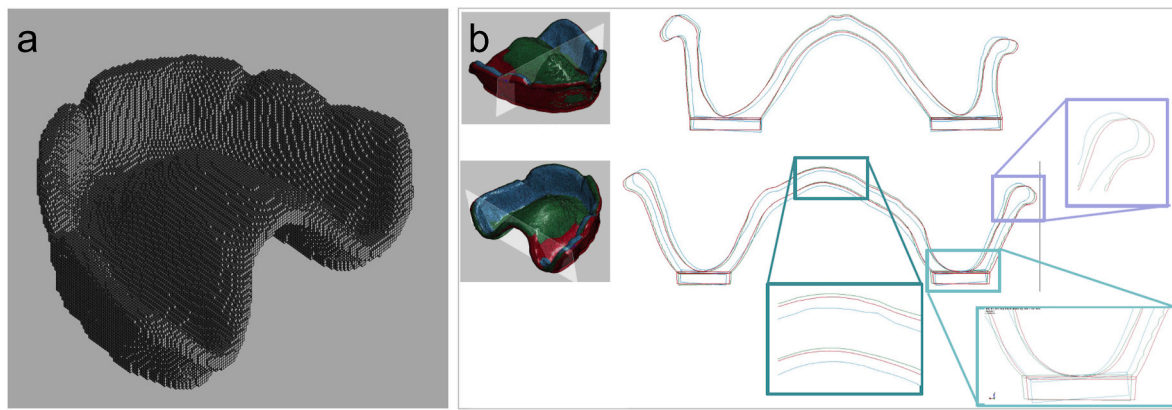


**Fig. 8.** (a) Visualization of the denture base as mesh for the simulation (PP-TM); (b) original target (red line) of the denture base; warped shaped (no optimization; blue line), and warped shape (optimized, green line).

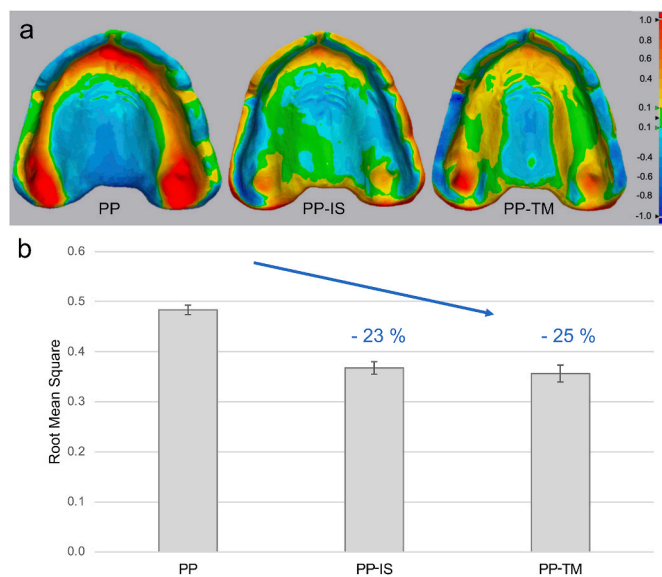


**Fig. 9.** (a) Exemplary visualization of deviations from CAD file of simulation-based optimized denture bases PP-IS and PP-TM in comparison to PP (not optimized). (b) Root Mean Square Values of optimized denture bases applying the PP-IS and PP-TM model in comparison to PP (not optimized). Error bars visualize the standard deviation. (color artwork).

annealing at 80 °C (Malpass and Band, 2012; Ehrenstein, 2011; Burkhardt et al., 2020).

BE showed a rather large increase in warpage despite its small increase in crystallinity in the DSC analysis during the sterilization process indicating that the elevated temperature of steam sterilization essentially releases inherent material stresses from molecular reorganization that have a significant macroscopic influence on warpage for the blend of biocopolyesters with a glass transition temperature above room temperature. PLA-based materials have been observed to exhibit similar heat deflection during steam sterilization in other studies (Burkhardt et al., 2022a,b; Chen et al., 2020). Furthermore, the present study showed that AR, which is also approved for the use of surgical guides, cannot be reliably sterilized maintaining stable dimensions at 134 °C using the standard steam sterilization protocol. This finding aligns with the manufacturer's recommendation to apply "gamma sterilization using a dose of 25–50 kGy" or "steam sterilization for 4 min at 132 °C with fractionated pre-vacuum" (Stratasys), which, however, limits a straightforward in-house sterilization at several clinics and most private practices and highlights the need for comprehensive material evaluation

and material design for medical AM applications. The two extrusion-based materials, which showed the greatest increase in warpage at 134 °C sterilization, were additionally examined at 121 °C steam sterilization. Both PP-GF and BE showed a lower increase in warpage at 121 °C compared to 134 °C, although the increase was still statistically significant for PP-GF due to a slightly increased crystallinity of the predominantly amorphous rubber phase as demonstrated via DSC analysis. Several studies investigated printed objects for their sterilizability at only 121 °C (Marei et al., 2019; Pieralli et al., 2020; Sharma et al., 2020; Rothlauf et al., 2023). However, the present study mainly focused on the sterilization protocol at 134 °C, since this protocol was frequently used in dental clinics due to its shorter time required for sterilization. Other mild sterilization protocols (e.g., H<sub>2</sub>O<sub>2</sub> plasma sterilization) do not appear to be suitable for daily use due to significantly higher costs (Adler et al., 1998). Nevertheless, it was shown that hydrostatic high pressure sterilization as an alternative sterilization method, can even lead to improved mechanical properties of the polymers, while traditional steam sterilization often causes reduced mechanical characteristics, deformation, and surface damage (Linares-Alvelais et al., 2018). An alternative method to obtain sterile FFF printed parts with fine structures might be inherent sterilization, where a high printing temperature is applied under sterile printing conditions (Neijhoft et al., 2023).

Furthermore, a significant influence of the geometry of the printed objects on the dimensional sterilizability was observed. Although sterilization of the denture bases showed a significant increase of the root mean square (RMS) value, the increase was fairly similar and moderate for all of the evaluated materials. This effect can be attributed to the fact that the denture bases are thicker and stiffer compared to the square specimens, resulting in an overall decreased thermal deformation during sterilization (Burkhardt et al., 2022a,b). This observation was consistent with a recent study where FFF-printed thin PLA structures below 5 mm showed massive deformations during steam sterilization, whereas thicker parts could be sterilized using steam sterilization at 121 °C for 20 min (Neijhoft et al., 2023). The results of the present study indicated that the most pronounced deformation during sterilization was present in the dorsal marginal areas of the denture bases, comparable to the warpage pattern of the square specimens, which showed the most severe warpage in the corner areas. In this case, warpage occurs at the end of the longest printed axis when the shrinkage of the polymer was parallel to it (Schirmeister et al., 2021). Given that these square specimens are particularly prone to warpage and shrinkage due to the thin, long axes, they allowed for an accurate warpage quantification of the evaluated materials (Spoerk et al., 2017). In another study, which examined the same geometry, one corner of the square specimen was subjected to a certain force and the height of the opposite corner was measured (Schirmeister et al., 2021). In this study, the volume below the squares

was determined using a coordinate measuring machine. The accuracy depends on the number of points measured. With the scanner used, 16 million points were measured to achieve an accuracy of  $\pm 10 \mu\text{m}$  and a repeatability of  $2 \mu\text{m}$  (Keyence, 2024). Other methods for precise measurement of dimensional accuracy can also be  $\mu\text{-CT}$  scans, which also allow the analysis of the porosity of the test specimens (Vidakis et al., 2022a, 2023). The determination of dimensional accuracy using CT scans as well as coordinate measuring machines is described as reliable in the literature (Vidakis et al., 2022a, 2023; Villarraga-Gómez et al., 2018; Warnett et al., 2016).

The PP material proved to be particularly resistant to thermal and chemical influences due to its increased crystalline properties, making the evaluated filament suitable for a wide range of applications. In addition to dentures, surgical guides or surgical instruments could be possible clinical applications. However, for a clinical application, further reduction of warpage during the cooling process after AM is necessary. One possible approach is to simulate the CAD file to compensate for inherent warpage issues of the material (Syrlybayev et al., 2021). The process simulation input included part geometry, thermomechanical material properties, AM parameters such as nozzle, build plate and chamber temperature, as well as print path and cooling conditions. Two different models for simulation-based optimization of the denture base were generated (PP-IS; PP-TM). As these models were based on different assumptions and approaches, slight differences in their predictions are expected, especially at local level, as confirmed by the parts printed from the compensated target geometries generated by the two models. The PP-TM model, with its more complex and detailed modeling of the interaction between the deposited layers and the ability to account for relaxation effects, was assumed to be more reliable and accurate. However, the improvement in the dimensional accuracy of the denture base with PP-TM approach was only slightly compared to PP-IS. This could be influenced by the accuracy of the input data describing the thermomechanical properties of the material.

Further improvements can be achieved by using tailored material testing to generate input material parameters and adopting a more accurate model for the description of the process. Incorporating a detailed crystallization model may also enhance the accuracy of the simulation, although some aspects related to crystallization are already phenomenologically and implicitly considered in the input data. Despite the approximations in the present evaluation, the findings offer interesting possibilities for designers, reducing the need for time-consuming experimental tests and leading to a significant reduction of warpage with only minor computational effort. One limitation in the present simulation lies in the modelling of the annealing phase occurring at the end of the printing, as it was not carried out at the experimental temperature value due to some limitation in the current release of the software. Higher accuracy in the simulation is expected to be achieved once the annealing phase will be reproduced more faithful in future software releases.

Although the increased dimensional accuracy induced by fillers and additives has been described in the literature (Winter et al., 2022), the advantage of simulation-based optimization is that the material composition of a medically approved material does not have to be changed and the settings used for the FFF can be retained. The results showed a clear tendency towards reduced deviation from the CAD file for both models, with minimal differences between the two. Therefore, for clinical applications, such as a denture base, reduced warpage during the printing process can be achieved with a simulation-based optimization of the CAD file, allowing for the extension of the range of materials for medical AM, particularly the applications of more versatile, chemically and mechanically resistant, and biocompatible polyolefins.

## 5. Conclusions

Within the limitations of this study, the following conclusions can be drawn.

- PP showed the highest warpage due to crystallization during cooling after AM compared to the other investigated extrusion-based materials PP-GF and BE as well as the photopolymerizing resin AR.
- All tested materials showed an increase in warpage of the square specimens and dentures after steam sterilization, whereby PP showed a comparatively small increase in warpage.
- An influence of the geometry on the dimensional stability was observed, since the dentures showed less warpage than the square specimens.
- However, for clinical application of the dentures, a reduced warpage during the printing process is necessary, to which simulation-based optimization of the CAD file can contribute.
- In future studies, further relevant geometries such as surgical guides should be evaluated after extrusion-based printing and their dimensionally accurate fabrication should be optimized using simulation-based optimization.

## Funding

This research did not receive any specific grant from funding agencies in the public, commercial, or not-profit sector.

## Data statement

Data will be made available on request.

## CRediT authorship contribution statement

**Felix Burkhardt:** Writing – original draft, Visualization, Supervision, Methodology, Investigation, Data curation, Conceptualization. **Carl G. Schirmeister:** Writing – review & editing, Software, Resources, Methodology, Data curation, Conceptualization. **Christian Wesemann:** Writing – review & editing, Software, Methodology. **Lukas Baur:** Writing – review & editing, Visualization, Investigation, Data curation. **Kirstin Vach:** Writing – review & editing, Formal analysis. **Massimo Nutini:** Writing – review & editing, Software, Methodology, Investigation, Data curation. **Erik H. Licht:** Writing – review & editing, Validation, Resources. **Marc C. Metzger:** Writing – review & editing, Conceptualization. **Rolf Mülhaupt:** Writing – review & editing, Supervision. **Benedikt C. Spies:** Writing – review & editing, Validation, Resources, Methodology, Conceptualization.

## Declaration of competing interest

The authors declare that they have no known competing financial interests or personal relationships that could have appeared to influence the work reported in this paper.

## Data availability

Data will be made available on request.

## Acknowledgements

Funded by the Berta-Ottenstein-Programme for Clinician Scientists, Faculty of Medicine, University of Freiburg.

## References

- Adler, S., Scherrer, M., Daschner, F.D., 1998. Costs of low-temperature plasma sterilization compared with other sterilization methods. *J. Hosp. Infect.* 40, 125–134. [https://doi.org/10.1016/S0195-6701\(98\)90091-3](https://doi.org/10.1016/S0195-6701(98)90091-3).
- Aimar, A., Palermo, A., Innocenti, B., 2019. The role of 3D printing in medical applications: a state of the art. *J. Healthcare Eng.* 1–10. <https://doi.org/10.1155/2019/5340616>, 2019.
- Bachhar, N., Gudadhe, A., Kumar, A., Andrade, P., Kumaraswamy, G., 2020. 3D printing of semicrystalline polypropylene: towards eliminating warpage of printed objects. *Bull. Mater. Sci.* 43, 171. <https://doi.org/10.1007/s12034-020-02097-4>.



- Ballard, D.H., Mills, P., Duszak, R., Weisman, J.A., Rybicki, F.J., Woodard, P.K., 2020. Medical 3D printing cost-savings in orthopedic and maxillofacial surgery: cost analysis of operating room time saved with 3D printed anatomic models and surgical guides. *Acad. Radiol.* 27, 1103–1113. <https://doi.org/10.1016/j.acra.2019.08.011>.
- Bertolino, M., Battagazzore, D., Arrigo, R., Frache, A., 2021. Designing 3D printable polypropylene: material and process optimisation through rheology. *Addit. Manuf.* 40, 101944 <https://doi.org/10.1016/j.addma.2021.101944>.
- Burkhardt, F., Schirmeister, C.G., Wesemann, C., Nutini, M., Pieralli, S., Licht, E.H., Metzger, M., Wenz, F., Mülhaupt, R., Spies, B.C., 2020. Pandemic-driven development of a medical-grade, economic and decentralized applicable polyolefin filament for additive fused filament fabrication. *Molecules* 25, 5929. <https://doi.org/10.3390/molecules25245929>.
- Burkhardt, F., Schmidt, V.D., Wesemann, C., Schirmeister, C.G., Rothlauf, S., Pieralli, S., Brandenburg, L.S., Kleinvogel, L., Vach, K., Spies, B.C., 2022a. Tailoring the composition of biocopolyester blends for dimensionally accurate extrusion-based printing, annealing and steam sterilization. *Sci. Rep.* 12, 20341 <https://doi.org/10.1038/s41598-022-24991-z>.
- Burkhardt, Felix, Spies, B.C., Wesemann, C., Schirmeister, C.G., Licht, E.H., Beuer, F., Steinberg, T., Pieralli, S., 2022b. Cytotoxicity of polymers intended for the extrusion-based additive manufacturing of surgical guides. *Sci. Rep.* 12, 7391. <https://doi.org/10.1038/s41598-022-11426-y>.
- Carneiro, O.S., Silva, A.F., Gomes, R., 2015. Fused deposition modeling with polypropylene. *Mater. Des.* 83, 768–776. <https://doi.org/10.1016/j.matdes.2015.06.053>.
- Chen, J.V., et al., 2020. Identifying a commercially-available 3D printing process that minimizes model distortion after annealing and autoclaving and the effect of steam sterilization on mechanical strength. *3D Print. Med.* 6, 9. <https://doi.org/10.1186/s41205-020-00062-9>.
- Chung, T.C.M., 2013. Functional polyolefins for energy applications. *Macromolecules* 46, 6671–6698. <https://doi.org/10.1021/ma401244t>.
- Davis, C.S., Hillgartner, K.E., Han, S.H., Seppala, J.E., 2017. Mechanical strength of welding zones produced by polymer extrusion additive manufacturing. *Addit. Manuf.* 16, 162–166. <https://doi.org/10.1016/j.addma.2017.06.006>.
- Deng, K., Chen, H., Wei, W., Wang, X., Sun, Y., 2023. Accuracy of tooth positioning in 3D-printing aided manufactured complete dentures: an in vitro study. *J. Dent.* 131, 104459 <https://doi.org/10.1016/j.jdent.2023.104459>.
- Díez-Rodríguez, T.M., Blázquez-Blázquez, E., Pérez, E., Cerrada, M.L., 2020. Composites Based on Poly(Lactic Acid) (PLA) and SBA-15: effect of mesoporous silica on thermal stability and on isothermal crystallization from either glass or molten state. *Polymers* 12, 2743. <https://doi.org/10.3390/polym12112743>.
- Ehrenstein, G.W., 2011. *Polymer-Werkstoffe: Struktur - Eigenschaften - Anwendung*, 3. Aufl. Hanser, München.
- EN 13432, 2002. *Packaging - requirements for packaging recoverable through composting and biodegradation - test scheme and evaluation criteria for the final acceptance of packaging*. Digimat Documentation Release. e-Xstream engineering, 2021.
- Fischer, J.M., 2013. *Handbook of molded part shrinkage and warpage*. In: *Plastics Design Library*, second ed. Elsevier/William Andrew, Amsterdam.
- Gielisch, M., Heimes, D.G.E., Thiem, D., Boesing, C., Krumpoltz, M., Al-Nawas, B.W., Kämmerer, P., 2022. Steam-sterilized and degradable fused filament fabrication-printed polylactide/polyhydroxyalkanoate surgical guides for dental implants: are they accurate enough for static navigation? *Int J. Bioprint.* 9 <https://doi.org/10.18063/ijb.v9i2.655>.
- Hada, T., Komagamine, Y., Kanazawa, M., Minakuchi, S., 2023. Fabrication of sports mouthguards using a semi-digital workflow with 4D-printing technology. *J. Prosthodont. Res.* JPR\_D\_22\_00274. [https://doi.org/10.2186/jpr.JPR\\_D\\_22\\_00274](https://doi.org/10.2186/jpr.JPR_D_22_00274).
- Hoang, D., Perrault, D., Stevanovic, M., Ghiassi, A., 2016. Surgical applications of three-dimensional printing: a review of the current literature & how to get started. *Ann. Transl. Med.* 4 <https://doi.org/10.21037/atm.2016.12.18>, 456–456.
- Kaynak, B., Spoerk, M., Shirole, A., Ziegler, W., Sapkota, J., 2018. Polypropylene/cellulose composites for material extrusion additive manufacturing. *Macromol. Mater. Eng.* 303, 1800037 <https://doi.org/10.1002/mame.201800037>.
- Keyence, 2024. 3D Scanner CMM Controller VL-500 [WWW Document]. <https://www.keyence.com/products/measure-sys/3d-scanner/vl/models/vl-500/>. (Accessed 28 February 2024). <https://www.keyence.com/products/measure-sys/3d-scanner/vl/models/vl-500/>.
- Liao, Y., Liu, C., Coppola, B., Barra, G., Di Maio, L., Incarnato, L., Lafdi, K., 2019. Effect of porosity and crystallinity on 3D printed PLA properties. *Polymers* 11, 1487. <https://doi.org/10.3390/polym11091487>.
- Ligon, S.C., Liska, R., Stampf, J., Gurr, M., Mülhaupt, R., 2017. Polymers for 3D printing and customized additive manufacturing. *Chem. Rev.* 117, 10212–10290. <https://doi.org/10.1021/acs.chemrev.7b00074>.
- Linares-Alvelais, J., Figueroa-Cavazos, J., Chuck-Hernandez, C., Siller, H., Rodríguez, C., Martínez-López, J., 2018. Hydrostatic high-pressure post-processing of specimens fabricated by DLP, SLA, and FDM: an alternative for the sterilization of polymer-based biomedical devices. *Materials* 11, 2540. <https://doi.org/10.3390/ma11122540>.
- Lüchtenborg, J., Burkhardt, F., Nold, J., Rothlauf, S., Wesemann, C., Pieralli, S., Wemken, G., Witkowski, S., Spies, B.C., 2021. Implementation of fused filament fabrication in dentistry. *Appl. Sci.* 11, 6444. <https://doi.org/10.3390/app11146444>.
- Ma, B., Park, T., Chun, I., Yun, K., 2018. The accuracy of a 3D printing surgical guide determined by CBCT and model analysis. *J. Adv. Prosthodont.* 10, 279. <https://doi.org/10.4047/jap.2018.10.4.279>.
- Malpass, D.B., Band, E.I., 2012. *Introduction to Industrial Polypropylene: Properties, Catalysts, Processes*. John Wiley & Sons ; Scrivener Pub, Hoboken, N.J. Salem, Mass.
- Marei, H.F., Alshaha, A., Alarifi, S., Almasoud, N., Abdelhady, A., 2019. Effect of steam heat sterilization on the accuracy of 3D printed surgical guides. *Implant Dent.* 28, 372–377. <https://doi.org/10.1097/ID.0000000000000908>.
- Mohan, N., Senthil, P., Vinodh, S., Jayanth, N., 2017. A review on composite materials and process parameters optimisation for the fused deposition modelling process. *Virtual Phys. Prototyp.* 12, 47–59. <https://doi.org/10.1080/17452759.2016.1274490>.
- Moutsopoulou, A., Petousis, M., Michailidis, N., Mountakis, N., Argyros, A., Papadakis, V., Spiridaki, M., Charou, C., Ntintakis, I., Vidakis, N., 2023. Optimization of isotactic polypropylene nanocomposite content of tungsten carbide for material extrusion 3D printing. *J. Compos. Sci.* 7, 393. <https://doi.org/10.3390/jcs7090393>.
- Mülhaupt, R., 2013. Green polymer chemistry and bio-based plastics: dreams and reality. *Macromol. Chem. Phys.* 214, 159–174. <https://doi.org/10.1002/macp.201200439>.
- Musib, M.K., 2012. A review of the history and role of UHMWPE as A component in total joint replacements. *Int. J. Biol. Eng.* 1, 6–10. <https://doi.org/10.5923/j.ijbe.20110101.02>.
- Nath, P., Olson, J.D., Mahadevan, S., Lee, Y.-T.T., 2020. Optimization of fused filament fabrication process parameters under uncertainty to maximize part geometry accuracy. *Addit. Manuf.* 35, 101331 <https://doi.org/10.1016/j.addma.2020.101331>.
- Neijhoft, J., Henrich, D., Kammerer, A., Janko, M., Frank, J., Marzi, I., 2023. Sterilization of PLA after fused filament fabrication 3D printing: evaluation on inherent sterility and the impossibility of autoclaving. *Polymers* 15, 369. <https://doi.org/10.3390/polym15020369>.
- Németh, A., Vitai, V., Czumbel, M.L., Szabó, B., Varga, G., Kerémi, B., Hegyi, P., Hermann, P., Borbély, J., 2023. Clear guidance to select the most accurate technologies for 3D printing dental models – a network meta-analysis. *J. Dent.* 134, 104532 <https://doi.org/10.1016/j.jdent.2023.104532>.
- Park, S.-D., Todo, M., Arakawa, K., 2004. Effect of annealing on the fracture toughness of poly(lactic acid). *J. Mater. Sci.* 39, 1113–1116. <https://doi.org/10.1023/B:JMSS.0000012957.02434.1e>.
- Petousis, M., Michailidis, N., Papadakis, V., Mountakis, N., Argyros, A., Spiridaki, M., Moutsopoulou, A., Nasikas, N.K., Vidakis, N., 2023. The impact of the glass microparticles features on the engineering response of isotactic polypropylene in material extrusion 3D printing. *Mater. Today Commun.* 37, 107204 <https://doi.org/10.1016/j.mtcomm.2023.107204>.
- Pieralli, S., Spies, B.C., Hromadnik, V., Nicic, R., Beuer, F., Wesemann, C., 2020. How accurate is oral implant installation using surgical guides printed from a degradable and steam-sterilized biopolymer? *J. Clin. Dent.* 9, 2322. <https://doi.org/10.3390/jcm9082322>.
- Revilla-León, M., Sadeghpour, M., Özcan, M., 2020. An update on applications of 3D printing technologies used for processing polymers used in implant dentistry. *Odontology* 108, 331–338. <https://doi.org/10.1007/s10266-019-00441-7>.
- Rothlauf, S., Pieralli, S., Wesemann, C., Burkhardt, F., Vach, K., Kernen, F., Spies, B.C., 2023. Influence of planning software and template design on the accuracy of static computer assisted implant surgery performed using guides fabricated with material extrusion technology: an in vitro study. *J. Dent.* 132, 104482 <https://doi.org/10.1016/j.jdent.2023.104482>.
- Schirmeister, C.G., Schächtele, S., Keßler, Y., Hees, T., Köhler, R., Schmitz, K., Licht, E.H., Muelhaupt, R., 2021. Low warpage nanophase-separated polypropylene/olefinic elastomer reactor blend composites with digitally tuned glass fiber orientation by extrusion-based additive manufacturing. *ACS Appl. Polym. Mater.* 3, 2070–2081. <https://doi.org/10.1021/acscapm.1c00119>.
- Schmutzler, C., Zimmermann, A., Zaeh, M.F., 2016. Compensating warpage of 3D printed parts using free-form deformation. *Procedia CIRP* 41, 1017–1022. <https://doi.org/10.1016/j.procir.2015.12.078>.
- Schubert, O., Edelhoff, D., Erdelt, K., Nold, E., Güth, J.-F., 2022. Accuracy of surface adaptation of complete denture bases fabricated using milling, material jetting, selective laser sintering, digital light processing, and conventional injection molding. *Int. J. Comput. Dent.* 25, 151–159. <https://doi.org/10.3290/j.ijcd.b2588131>.
- Sharma, A., Tiwari, S., Deb, M.K., Marty, J.L., 2020. Severe acute respiratory syndrome coronavirus-2 (SARS-CoV-2): a global pandemic and treatment strategies. *Int. J. Antimicrob. Agents* 56, 106054. <https://doi.org/10.1016/j.ijantimicag.2020.106054>.
- Spoerk, M., Holzer, C., Gonzalez-Gutierrez, J., 2020. Material extrusion-based additive manufacturing of polypropylene: a review on how to improve dimensional inaccuracy and warpage. *J. Appl. Polym. Sci.* 137, 48545 <https://doi.org/10.1002/app.48545>.
- Spoerk, M., Sapkota, J., Weingrill, G., Fischinger, T., Arbeiter, F., Holzer, C., 2017. Shrinkage and warpage optimization of expanded-perlite-filled polypropylene composites in extrusion-based additive manufacturing. *Macromol. Mater. Eng.* 302, 1700143 <https://doi.org/10.1002/mame.201700143>.
- Spoerk, M., Savandaiah, C., Arbeiter, F., Sapkota, J., Holzer, C., 2019. Optimization of mechanical properties of glass-spheres-filled polypropylene composites for extrusion-based additive manufacturing. *Polym. Compos.* 40, 638–651. <https://doi.org/10.1002/pc.24701>.
- Stratasys, n.d. [https://www.stratasys.com/siteassets/materials/materials-catalog/biocompatable/mds\\_pj\\_med610\\_0720a.pdf?v=48e364](https://www.stratasys.com/siteassets/materials/materials-catalog/biocompatable/mds_pj_med610_0720a.pdf?v=48e364). [WWW Document]. URL (accessed May.31.2023)..
- Stürzel, M., Mihan, S., Mülhaupt, R., 2016. From multisite polymerization catalysis to sustainable materials and all-polyolefin composites. *Chem. Rev.* 116, 1398–1433. <https://doi.org/10.1021/acs.chemrev.5b00310>.
- Syrylybayev, D., Zharylkassyn, B., Seisekulova, A., Perveen, A., Talamona, D., 2021. Optimization of the warpage of fused deposition modeling parts using finite element method. *Polymers* 13, 3849. <https://doi.org/10.3390/polym13213849>.

- Tabone, M.D., Cregg, J.J., Beckman, E.J., Landis, A.E., 2010. Sustainability metrics: life cycle assessment and green design in polymers. *Environ. Sci. Technol.* 44, 8264–8269. <https://doi.org/10.1021/es101640n>.
- Vidakis, N., David, C., Petousis, M., Sagris, D., Mountakis, N., 2023. Optimization of key quality indicators in material extrusion 3D printing of acrylonitrile butadiene styrene: the impact of critical process control parameters on the surface roughness, dimensional accuracy, and porosity. *Mater. Today Commun.* 34, 105171 <https://doi.org/10.1016/j.mtcomm.2022.105171>.
- Vidakis, N., David, C., Petousis, M., Sagris, D., Mountakis, N., Moutsopoulou, A., 2022a. The effect of six key process control parameters on the surface roughness, dimensional accuracy, and porosity in material extrusion 3D printing of polylactic acid: prediction models and optimization supported by robust design analysis. *Adv. Indust. Manuf. Eng.* 5, 100104 <https://doi.org/10.1016/j.aime.2022.100104>.
- Vidakis, N., Petousis, M., Tzounis, L., Maniadi, A., Velidakis, E., Mountakis, N., Papageorgiou, D., Liebscher, M., Mechtcherine, V., 2020a. Sustainable additive manufacturing: mechanical response of polypropylene over multiple recycling processes. *Sustainability* 13, 159. <https://doi.org/10.3390/su13010159>.
- Vidakis, N., Petousis, M., Velidakis, E., Liebscher, M., Mechtcherine, V., Tzounis, L., 2020b. On the strain rate sensitivity of fused filament fabrication (FFF) processed PLA, ABS, PETG, PA6, and PP thermoplastic polymers. *Polymers* 12, 2924. <https://doi.org/10.3390/polym12122924>.
- Vidakis, N., Petousis, M., Velidakis, E., Mountakis, N., Fischer-Griffiths, P.E., Grammatikos, S.A., Tzounis, L., 2022b. Fused Filament Fabrication 3D printed polypropylene/alumina nanocomposites: effect of filler loading on the mechanical reinforcement. *Polym. Test.* 109, 107545 <https://doi.org/10.1016/j.polymertesting.2022.107545>.
- Vidakis, N., Petousis, M., Velidakis, E., Tzounis, L., Mountakis, N., Kechagias, J., Grammatikos, S., 2021a. Optimization of the filler concentration on fused filament fabrication 3D printed polypropylene with titanium dioxide nanocomposites. *Materials* 14, 3076. <https://doi.org/10.3390/ma14113076>.
- Vidakis, N., Petousis, M., Velidakis, E., Tzounis, L., Mountakis, N., Korlos, A., Fischer-Griffiths, P.E., Grammatikos, S., 2021b. On the mechanical response of silicon dioxide nanofiller concentration on fused filament fabrication 3D printed isotactic polypropylene nanocomposites. *Polymers* 13, 2029. <https://doi.org/10.3390/polym13122029>.
- Villarraga-Gómez, H., Lee, C., Smith, S.T., 2018. Dimensional metrology with X-ray CT: a comparison with CMM measurements on internal features and compliant structures. *Precis. Eng.* 51, 291–307. <https://doi.org/10.1016/j.precisioneng.2017.08.021>.
- Wang, C., Shi, Y.-F., Xie, P.-J., Wu, J.-H., 2021. Accuracy of digital complete dentures: a systematic review of in vitro studies. *J. Prosthet. Dent.* 125, 249–256. <https://doi.org/10.1016/j.prosdent.2020.01.004>.
- Wang, T.-M., Xi, J.-T., Jin, Y., 2007. A model research for prototype warp deformation in the FDM process. *Int. J. Adv. Des. Manuf. Technol.* 33, 1087–1096. <https://doi.org/10.1007/s00170-006-0556-9>.
- Warnett, J.M., Titarenko, V., Kiraci, E., Attridge, A., Lionheart, W.R.B., Withers, P.J., Williams, M.A., 2016. Towards in-process x-ray CT for dimensional metrology. *Meas. Sci. Technol.* 27, 035401 <https://doi.org/10.1088/0957-0233/27/3/035401>.
- Wemken, G., Spies, B.C., Pieralli, S., Adali, U., Beuer, F., Wesemann, C., 2020. Do hydrothermal aging and microwave sterilization affect the trueness of milled, additive manufactured and injection molded denture bases? *J. Mech. Behav. Biomed. Mater.* 111, 103975 <https://doi.org/10.1016/j.jmbbm.2020.103975>.
- Williams, M.L., Landel, R.F., Ferry, J.D., 1955. The temperature dependence of relaxation mechanisms in amorphous polymers and other glass-forming liquids. *J. Am. Chem. Soc.* 77, 3701–3707. <https://doi.org/10.1021/ja01619a008>.
- Winter, K., Wilfert, J., Häupler, B., Erlmann, J., Altstädt, V., 2022. Large scale 3D printing: influence of fillers on warp deformation and on mechanical properties of printed polypropylene components. *Macromol. Mater. Eng.* 307, 2100528 <https://doi.org/10.1002/mame.202100528>.